

Validation of VAMUCH for Binary Composites

Wenbin Yu*

Utah State University, Logan, Utah 84322-4130

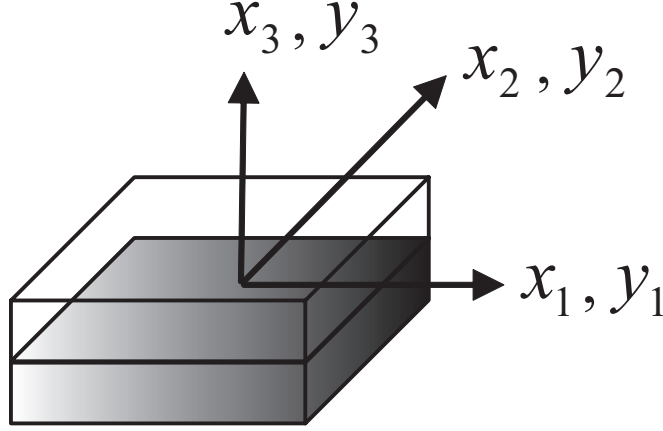


Figure 1. Sketch of a binary composite

We consider a periodic binary composite formed by orthotropic layers and the material axes are the same as the global coordinates x_i so that the material is uniform in the $x_1 - x_2$ plane and periodic along x_3 direction. A typical unit cell can be identified as shown in Figure 1, the dimension along y_3 is h and dimensions along y_1 and y_2 can be arbitrary. Let ϕ_1 and ϕ_2 denote the volume fractions of the first phase and the second phase, respectively, and we have $\phi_1 + \phi_2 = 1$. VAMUCH of this problem can be solved analytically. The strain energy density of the effective material can be obtained as:

$$\Pi_{\Omega} = \frac{1}{2} \begin{Bmatrix} \bar{\epsilon}_{11} \\ 2\bar{\epsilon}_{12} \\ \bar{\epsilon}_{22} \\ 2\bar{\epsilon}_{13} \\ 2\bar{\epsilon}_{23} \\ \bar{\epsilon}_{33} \end{Bmatrix}^T \begin{bmatrix} c_{11}^* & 0 & c_{13}^* & 0 & 0 & c_{16}^* \\ 0 & c_{22}^* & 0 & 0 & 0 & 0 \\ c_{13}^* & 0 & c_{33}^* & 0 & 0 & c_{36}^* \\ 0 & 0 & 0 & c_{44}^* & 0 & 0 \\ 0 & 0 & 0 & 0 & c_{55}^* & 0 \\ c_{16}^* & 0 & c_{36}^* & 0 & 0 & c_{66}^* \end{bmatrix} \begin{Bmatrix} \bar{\epsilon}_{11} \\ 2\bar{\epsilon}_{12} \\ \bar{\epsilon}_{22} \\ 2\bar{\epsilon}_{13} \\ 2\bar{\epsilon}_{23} \\ \bar{\epsilon}_{33} \end{Bmatrix} \quad (1)$$

It can be observed that the homogenized material properties still have the same orthotropic symmetry for this special case, although in general the homogenized material could be anisotropic, which means a fully

*Assistant Professor, Department of Mechanical and Aerospace Engineering

populated 6×6 stiffness matrix. The expressions of effective material properties c_{ij}^* are listed here.

$$\begin{aligned}
c_{11}^* &= \langle c_{11} \rangle - \frac{\phi_1 \phi_2 (c_{16}^{(2)} - c_{16}^{(1)})^2}{\phi_1 c_{66}^{(2)} + \phi_2 c_{66}^{(1)}} & c_{13}^* &= \langle c_{13} \rangle - \frac{\phi_1 \phi_2 (c_{16}^{(2)} - c_{16}^{(1)}) (c_{36}^{(2)} - c_{36}^{(1)})}{\phi_1 c_{66}^{(2)} + \phi_2 c_{66}^{(1)}} \\
c_{16}^* &= \frac{\phi_1 c_{16}^{(1)} c_{66}^{(2)} + \phi_2 c_{16}^{(2)} c_{66}^{(1)}}{\phi_1 c_{66}^{(2)} + \phi_2 c_{66}^{(1)}} & c_{33}^* &= \langle c_{33} \rangle - \frac{\phi_1 \phi_2 (c_{36}^{(2)} - c_{36}^{(1)})^2}{\phi_1 c_{66}^{(2)} + \phi_2 c_{66}^{(1)}} \\
c_{36}^* &= \frac{\phi_1 c_{36}^{(1)} c_{66}^{(2)} + \phi_2 c_{36}^{(2)} c_{66}^{(1)}}{\phi_1 c_{66}^{(2)} + \phi_2 c_{66}^{(1)}} \\
c_{66}^* &= 1 / \left\langle \frac{1}{c_{66}} \right\rangle & c_{55}^* &= 1 / \left\langle \frac{1}{c_{55}} \right\rangle & c_{44}^* &= 1 / \left\langle \frac{1}{c_{44}} \right\rangle & c_{22}^* &= \langle c_{22} \rangle
\end{aligned} \tag{2}$$

where the superscripted quantities are those from each phases of the composite. It can be observed that even for this simple case, only c_{22}^* is the same as the rule of mixture based on the Voigt hypothesis, and $c_{44}^*, c_{55}^*, c_{66}^*$ are the same as the rule of mixture based on the Reuss hypothesis. All the other components are different from these two rules of mixture. The effective material properties of the present theory reproduce those of a mathematical homogenization theory in Manevitch et al (2002). Using 2-noded line elements in VAMUCH, we can reproduce the analytical solution exactly (in the numerical sense).

For the purpose of illustration, let we consider both layers are isotropic materials with Young moduli as E_1 and E_2 , and Poisson's ratios as ν_1 and ν_2 , respectively. Let $E_1/E_2 = \rho_e$ and $\nu_1/\nu_2 = \rho_\nu$, different combinations of ρ_e and ρ_ν will be used here to study contribution of each constituents to the effective material properties.

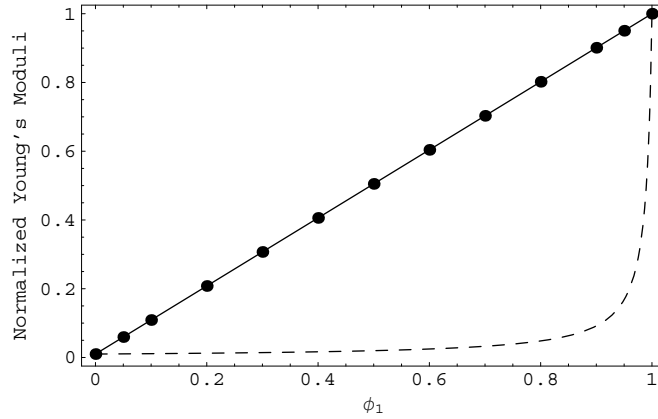


Figure 2. Effective in-plane Young's moduli predicted by different approaches. Dots: VAMUCH; solid line: Voigt's rule of mixture; dashed line: Reuss' rule of mixture.

First, let us study the case that Poisson's ratios of both materials are the same, say 0.3, and the first material is 100 times stiffer than the second material, *i.e.*, $\rho_\nu = 1$ and $\rho_e = 100$. We plot the Young's moduli and shear moduli normalized by E_1 and in Figures 2 - 5 with respect to the volume fraction of the stiff layer. We can find out that the in-plane Young's moduli (E_1^* and E_2^*) and in-plane shear moduli (G_{12}^*) obey Voigt's rule of mixture and transverse shear moduli (G_{13}^* and G_{23}^*) obey Reuss' rule of mixture. Although it seems that the transverse Young's modulus in Figure 6 also obey the Reuss's rule of mixture, in fact it is not as exposed in Figure 6. The difference between these two predictions are quite significant if ϕ_1 is not close to one. It is found that $\nu_{12}^*, \nu_{21}^*, \nu_{13}^*$, and ν_{23}^* are equal to 0.3 as could be predicted from the rules of mixtures, which means applying in-plane load will always get the same Poisson's effect as that of the constituent materials. However, ν_{31}^* and ν_{32}^* are not equal to 0.3 as shown in Figure 7. The binary

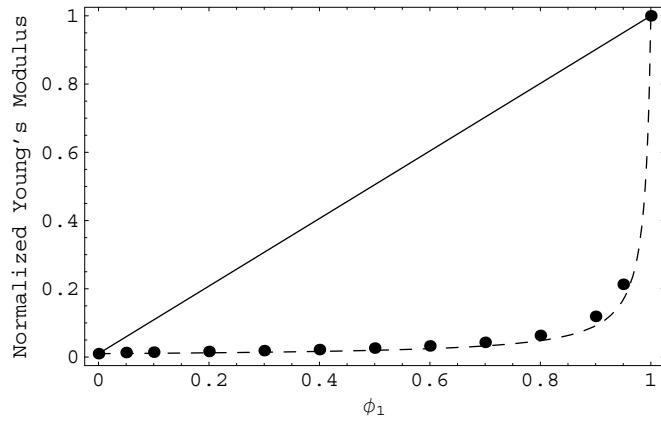


Figure 3. Effective transverse Young's modulus predicted by different approaches. Dots: VAMUCH; solid line: Voigt's rule of mixture; dashed line: Reuss' rule of mixture.

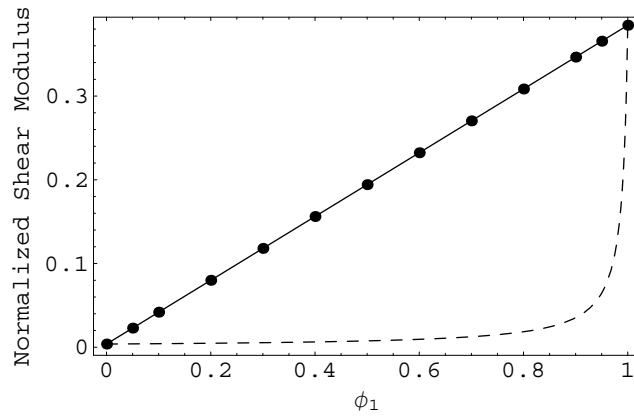


Figure 4. Effective in-plane shear modulus predicted by different approaches. Dots: VAMUCH; solid line: Voigt's rule of mixture; dashed line: Reuss' rule of mixture.

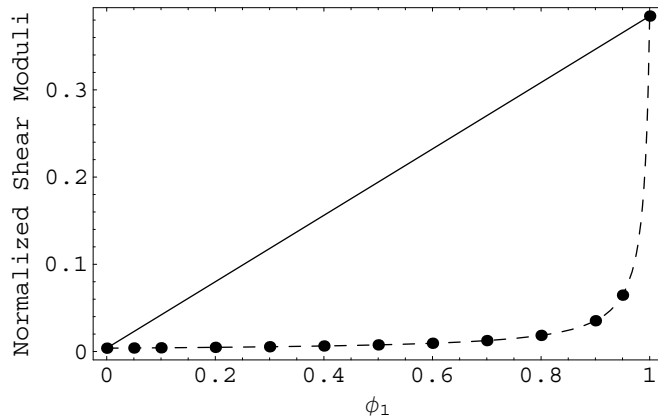


Figure 5. Effective transverse shear moduli predicted by different approaches. Dots: VAMUCH; solid line: Voigt's rule of mixture; dashed line: Reuss' rule of mixture.

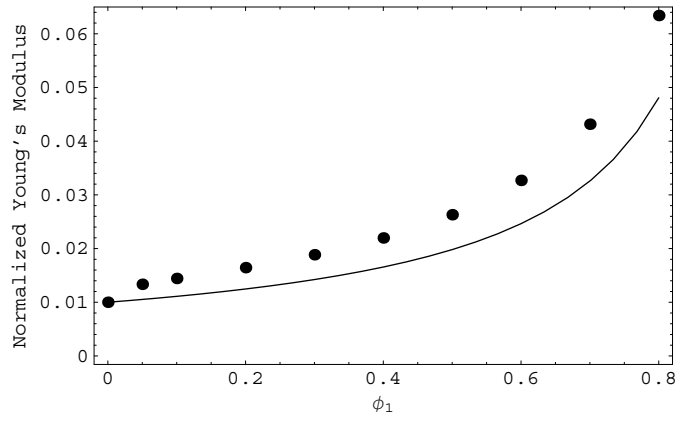


Figure 6. Effective transverse Young's modulus predicted by different approaches. Dots: VAMUCH; solid line: Reuss' rule of mixture.

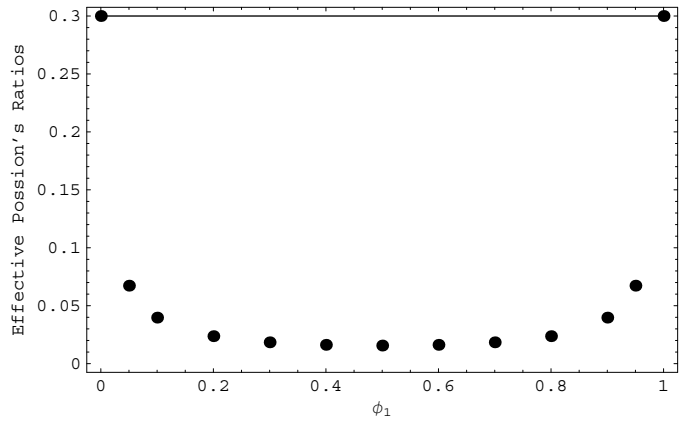


Figure 7. Effective Poisson's ratios (ν_{31}^* and ν_{32}^*) predicted by different approaches. Dots: VAMUCH; solid line: Voigt and Reuss rules of mixture.

composite material has very small Poisson's effect when the load is applied in the transverse direction and the volume fraction of stiff material varies between 0.2 and 0.8. This can be explained by the fact that during tension in transverse direction the soft layer will contribute mainly to the deformation and the stiff layer will restrain the lateral shrinkage of the material. Only if the restraining effect is small (*i.e.*, ϕ_1 is small) or the deformation contribution of the stiff layer becomes not negligible (*i.e.*, ϕ_1 is large), will the Poisson's ratios ν_{31}^* and ν_{32}^* approach that of the constituent materials.

Next, let us study the effect of mismatching Poisson's ratios. To this end, let us choose $\rho_e = 1$, $\nu_1 = 0.3$, and $\nu_2 = 0.06$. The prediction of in-plane Young's moduli ($E_1^* = E_2^*$, normalized by E_1) using different approaches are plotted in Figure 8. It is clear that VAMUCH predicts a value between the bounds provided by the rules of mixture as expected. The prediction of transverse Young's modulus (E_3^*) using VAMUCH is very close to the upper bound provided by the Voigt's rule of mixture as shown in Figure 9, while the Reuss' rule of mixture significantly under estimates this value. The in-plane shear modulus (G_{12}^*) obtained from VAMUCH is the same as that of Voigt's rule of mixture as shown in Figure 10, while the transverse shear moduli ($G_{13}^* = G_{23}^*$) is the same as that of Reuss's rule of mixture as shown in Figure 11. As far as the Poisson's ratios concerned, ν_{12}^* is the same as ν_{21}^* , ν_{13}^* is the same as ν_{23}^* , and ν_{31}^* is the same as ν_{32}^* . The Poisson's ratios predicted by different approaches are plotted in Figures 12, 13, and 14. It can be observed from this case that Poisson's ratios of constituent materials will affect the effective material properties even for isotropic materials with same Young's modulus. It is expected that this effect will be magnified for general anisotropic constituents.

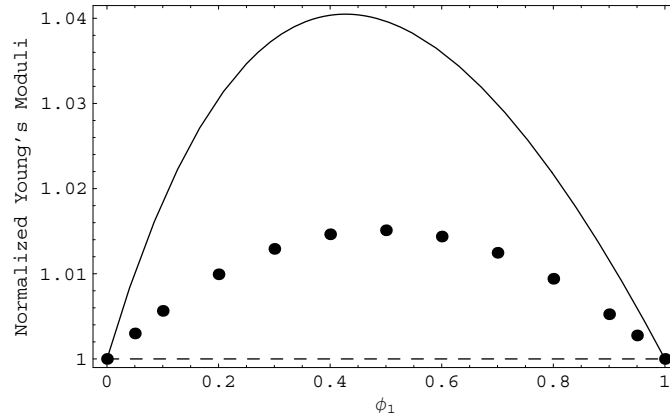


Figure 8. Effective in-plane Young's moduli predicted by different approaches. Dots: VAMUCH; regular dashed line: Voigt's rule of mixture; thick dashed line: Reuss' rule of mixture.

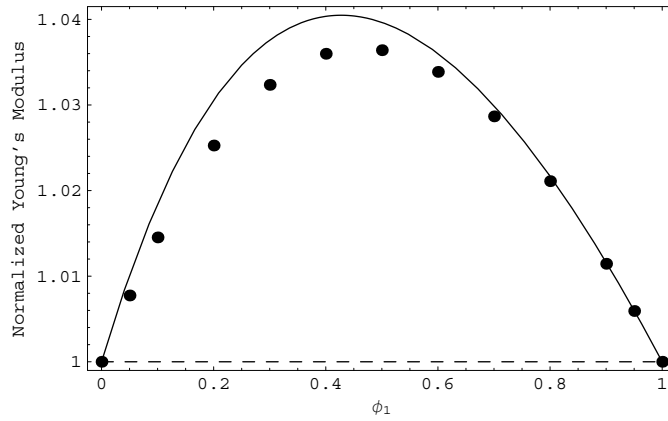


Figure 9. Effective transverse Young's modulus predicted by different approaches. Dots: VAMUCH; regular dashed line: Voigt's rule of mixture; thick dashed line: Reuss' rule of mixture.

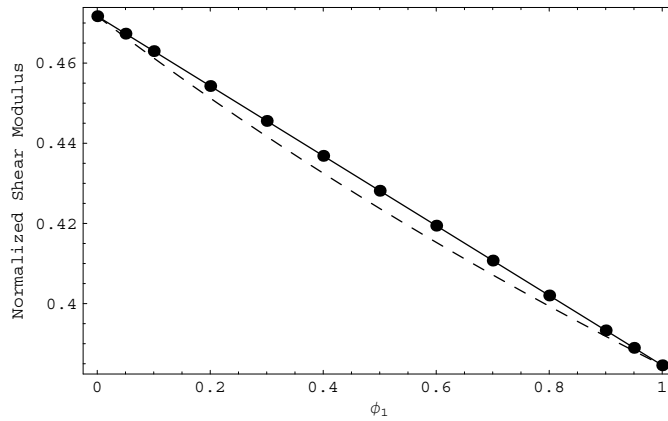


Figure 10. Effective in-plane shear modulus predicted by different approaches. Dots: VAMUCH; regular dashed line: Voigt's rule of mixture; thick dashed line: Reuss' rule of mixture.

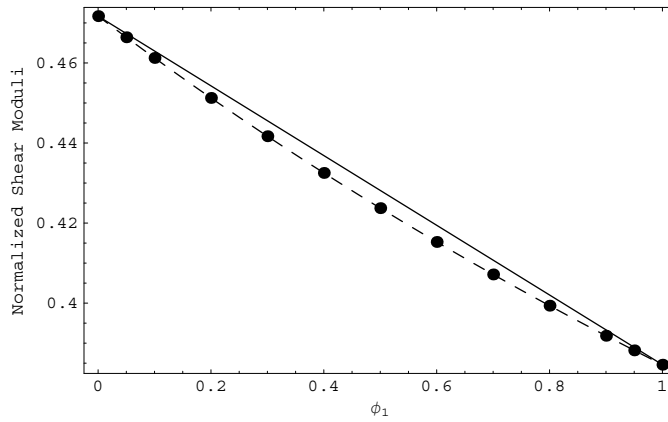


Figure 11. Effective transverse shear moduli predicted by different approaches. Dots: VAMUCH; regular dashed line: Voigt's rule of mixture; thick dashed line: Reuss' rule of mixture.

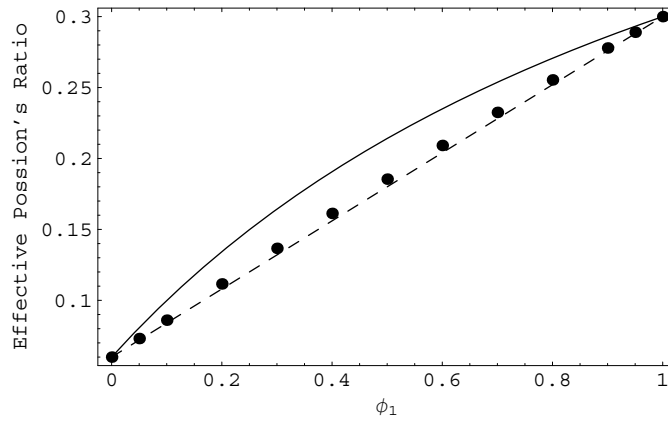


Figure 12. ν_{12}^* predicted by different approaches. Dots: VAMUCH; regular dashed line: Voigt's rule of mixture; thick dashed line: Reuss' rule of mixture.

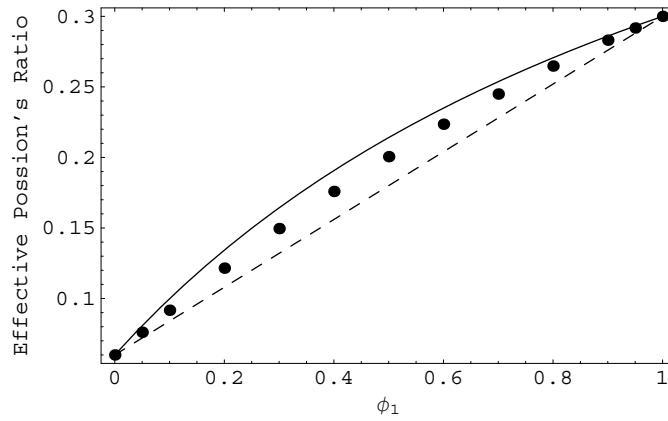


Figure 13. ν_{13}^* predicted by different approaches. Dots: VAMUCH; regular dashed line: Voigt's rule of mixture; thick dashed line: Reuss' rule of mixture.

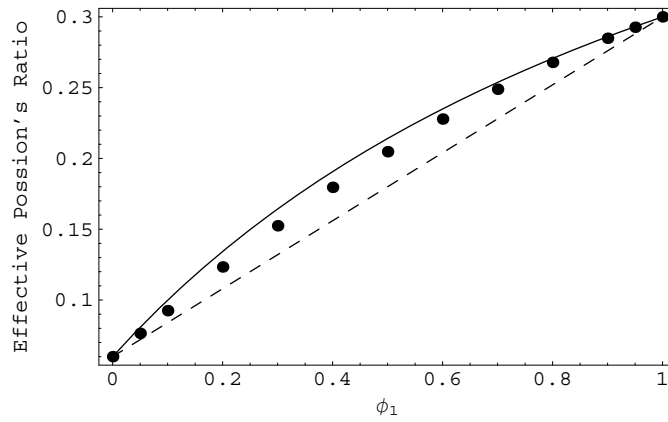


Figure 14. ν_{31}^* predicted by different approaches. Dots: VAMUCH; regular dashed line: Voigt's rule of mixture; thick dashed line: Reuss' rule of mixture.